The Report committee for Kunal Mukesh Raghuwansi certifies that this is the approved version of the following report:

Recent Techniques and Strategies in Development of High Mobility diketopyrrolopyrrole (DPP)-based Polymer for Organic Transistors

APPROVED BY

Supervisor: _____
Ananth Dodabalapur

_____
Sharath Hosali

Recent Techniques and Strategies in Development of High Mobility diketopyrrolopyrrole (DPP)-based Polymer for Organic Transistors

by

Kunal Mukesh Raghuwansi , B.S.

Report

Presented to the Faculty of the Graduate School
of the University of Texas at Austin
in Partial Fulfillment
of the Requirements
for the Degree of

Master of Science in Engineering

The University of Texas at Austin
May 2015

Recent Techniques and Strategies in Development of High Mobility diketopyrrolopyrrole (DPP)-based Polymer for Organic Transistors

by

Kunal Mukesh Raghuwansi, MSE

The University of Texas at Austin, 2015

SUPERVISOR: Ananth Dodabalapur

Abstract

For the past few years, organic field-effect transistors (OFETs) have attracted interest because of improvements in the charge carrier mobility and lifetime stability. OFETs based on π-conjugated polymers are of interest for complementary-like electronic circuits. A lot of research has been done on the development of a range of high-performance conjugated polymers with p-type, n-type, and ambipolar properties. One such material is diketopyrrolopyrrole (DPP)- based conjugated polymer. The electron deficient property of DPP, its planar backbone, and intermolecular hydrogen bonding results in materials with strong π- π stacking

interactions. It was found that the fused aromatic rings such as DPP and thieno[3,2-b]-thiophine form a large orbital overlapping area, which is useful for charge carrier transport. Similarly, applying side chain engineering and molecular design strategy by coupling diketopyrrolopyrrole with diketopyrrolopyrrole in an alternating fashion results in a copolymer with exceptional absorption characteristics (~1100 nm) and field effect mobility values of greater than 1 $cm^2V^{-1}s^{-1}$. DPP copolymerization with electron donor moieties, like thiophene, selenophene, naphthalene, bithiophene, benzothiadiazole, vinylene and thieno-thiophene, results in high charge carrier mobility. Moreover, the hole mobility higher than 10 $cm^2V^{-1}s^{-1}$ has been achieved based on donor-acceptor (D-A) copolymer with long hexadecyl side-chains. Thus, the high carrier mobility of DPP makes it an excellent candidate to obtain high performance OFETs for use in electronic circuits.

TABLE OF CONTENTS

List of Tables

List of Figures

semiconductors and (B) activation energies as a function of field-effect mobility in various polymer semiconductor-based transistors

Figure 12 (A) Chemical structures of the compounds used for the FOM study and (B) FOM as functions of channel length and field-effect mobility on various organics and polymers to compare the gate field-induced channel conductivity per unit gate voltage, extracted by a product of mobility and the relative dielectric constant of the gate insulator.

Figure 13 High electron mobility (up to 7.0 $cm^2\ V^{-1}\ s^{-1}$) is demonstrated with a diketopyrrolopyrrole (DPP)-based semiconductor (PDPP-CNTVT)

Figure 14 Transfer characteristics of ambipolar PDPP-TBT TFTs in top-, bottom-, and dual-gate modes.

Figure 15 Output characteristics for a typical ambipolar PTTDPP-BDT based OFET with aluminum electrodes.

Figure 16 OFET characteristics of the DPP derivatives: (a and b) output curves of (VGS = from 0 to 80 V with a step of 10 V) DPP-R16 and DPP-R18 thin-film based devices; (c and d) transfer curves (VGS = from 20 to 80 V at fixed VDS = 60 V) of DPP-R16 and DPP-R18 thin-film based devices respectively. (e) Output (V_{GS} = from 0 to -80 V with a step of -10 V) and (f) transfer (V_{GS} = from 20 to -80 V at fixed V_{DS} = -60 V) characteristic (I_{DS} vs. V_{DS}) curves of OFETs based on DPP-R18 1D-microwires and 650 nm thick polymer gate dielectric. The channel length and width of the OFETs were 20 and 2.7 um, respectively.

Figure 17 (a) Molecular structures of the three DPP derivatives used in this paper. Red dashed lines show where hydrogen bonds are formed with neighboring molecules. (b) Schematic of the OFET devices used in this study.

Figure 18 Transfer curves showing source–drain current (black traces), and gate leakage current (olive). Hole-enhanced devices shown in the column on the left were fabricated with Au source–drain electrodes, V_{SD} = -10 V in all cases. Electron-enhanced devices with Al source–drain electrodes are shown on the right, with V_{SD} = 10 V.

Introduction

OFETs based on conjugated polymer, oligomers, or fused aromatics have shown the promise to be an alternative source to more traditional transistors based on inorganic materials[1]. Continuous improvements of the charge carrier mobility have made polymeric semiconductors reach performances of amorphous silicon[2]. Semiconducting polymers can be processed from solution on roll to roll machinery for high throughput. Molecular ordering, molecular weight, growth mode and purity are some of the important properties of the polymer that affect its semiconducting properties. Producing mechanical shear in a solution of conjugated small molecules and polymers can improve the molecular orientation, film crystallinity and chain alignment that can help improve carrier mobility. A lot of attention has been focused on aspects concerning n-type charge transport and ambipolar charge transport in π conjugated materials. One important variable for achieving high carrier mobility is molecular weight (MW). Low MW material tend to form grain boundaries that can affect the carrier mobility[3]. Therefore, for high performance high molecular weight materials are required although, high MW materials tend to present difficulties during fabrication process. An alternate route to achieve high carrier mobility with respect to MW is under investigation. X-Ray techniques such as X-ray diffraction (XRD), grazing incidence X-ray diffraction (GIXD) and others have been

used to study the morphology and ordering of DPP-based materials[4].

Understanding of the molecular assembly process and the resulting short and long range order is important to advance organic electronics. In this context, DPP based polymers are showing the ability of displaying some of the highest mobilities (hole mobility > 10 $cm^2V^{-1}s^{-1}$) due to the aggregating properties of the DPP moieties. This report will summarize the different techniques utilized to improve the carrier mobilities of DPP based copolymers, highlight the relationship between the thin film morphology and the mobilities observed and investigating the charge transport behavior of the DPP based high mobility polymers to optimize the devices by lowering the operating voltage and removing hysteresis. Properties of Organic Thin Film Transistors (OTFTs) and performances of some of the most high mobility DPP-based compounds that are discussed in this report are summarized in Table 1.

Semiconducting Polymer Design

In order to have high charge mobility, it is important for the semiconducting polymer to have some kind of organized thin film microstructure. For FET devices, the most common way to achieve high charge transport is by having a coplanar conjugated backbone conformation with closely π stacked crystalline chains that form sheet-like lamellae[5]. Orienting the crystalline domains such that the planar backbone structures are orthogonal to the plane of the substrate can increase charge transport. Lamella structures with aromatic backbones vertically separated by insulating layers of alkyl chains extending from the backbone can form on long-range π stacks. Interlocking of side-chains between vertically adjacent lamellae can promote large domain sizes and improve ordering. This interlocking occurs when the side-chain density along a polymer chain is low enough to allow chains from the vertical lamella to occupy between the chains. Effect of shorter π – π stacking and improved molecular ordering is explained further with examples in the upcoming sections.

Fabrication

High crystalline semiconducting polymers in thin film transistors (TFTs) are usually fabricated using solution-processing technologies such as spin-coating, ink-jet printing, roll-to-roll processing, and drop-casting[6]. Thermally annealing the films at an appropriate temperature, results in higher degree of crystallinity and edge-on orientation of the polymer chains. However, thermally annealing films fabricated by solution-process techniques do not provide polymer-chain alignment that is suitable for enhancing the charge transport properties. One method that has been proposed produces mechanical shear in a solution of small molecules and polymers, improving film crystallinity, molecular orientation and chain alignment in the shearing direction as shown in the figure 1. Thus, this method increases the carrier mobility significantly compared to spin-coating methods. Template-assisted self-assembly method using poly-dimethylsiloxane (PDMS) mold helps confine small molecules to micro and nanospaces for self assembly and leads to formation of long range order in a specific direction[7]. Combining the process of both methods described above, "template-guided solution-shearing" (TGSS) was suggested by Jicheol Shin and group. This method aligns the polymer chains in a particular direction by increasing the contact area between the solution and the surface of the rectangular micro-grooves in the PDMS template (figure 1). Polymer chains in the prisms are aligned in the shearing direction by the PDMS template. PTDPP-DTTE polymer consisting of dithienyl-diketopyrrolopyrrole (DPP), thiophene and

thienothiophene units was used to fabricate the FETs.

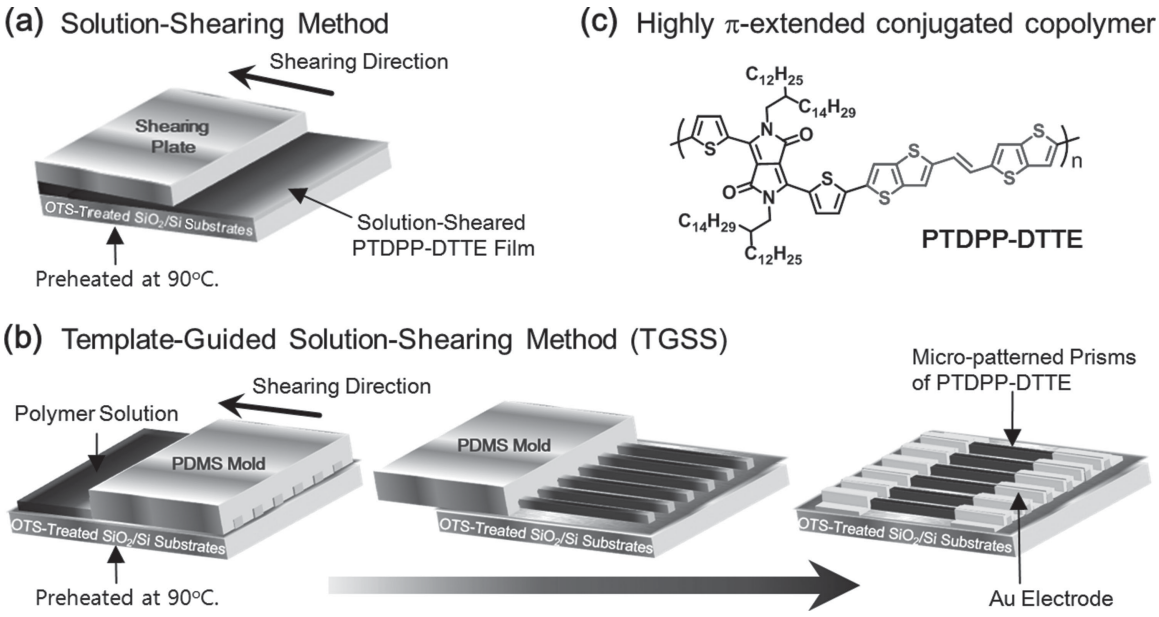

Figure 1 a) Solution-shearing method using a planar plate. b) Template-guided solution-shearing (TGSS) method using a PDMS mold with uniaxially aligned microgrooves. c) Chemical structure of PTDPP-DTTE [7]

PTDPP-DTTE with molecular weight (MW) of 127.85 kDa, has very long and bulky dodecylhexadecyl side chains with and optical bandgap of 1.31eV. GI-XRD results showed that thermally annealed PTDPP-DTTE films exhibited dense crystallite geometry and an edge-on orientation of the polymer chains, both of which lead to an increased carrier transport within the film [7]. TFT made with a thermally annealed sheared film exhibited a mobility of 4.77 $cm^2\ V^{-1}\ s^{-1}$ and a high on/off current ratio in air, which is much higher than spin coated annealed film. AFM analysis demonstrated that solution-shearing method controls the direction of polymer chain alignment along the shearing direction, which meant that the surface

topography was important. Moreover, solution-shearing process combined with TGSS can provide high degree of anisotropy of the polymer chains and promote a greater degree of alignment among the polymer chains.

Figure 2a shows an image of FET device with micro-patterned prism channels formed from TGSS using a PDMS template. High magnification image of the surface topography can be seen in figure 2b. A maximum mobility of 7.43 $cm^2\ V^{-1}\ s^{-1}$ and a high on/off current ratio (>10^5) was achieved with FETs that had annealed prism channels. Transfer and output curves of FETs fabricated with TGSS micro-patterned prisms are shown in figures 2d and 2e. π−π-stacking distance calculated using GI-XRD was about 3.47 Å in prisms, which is lower than spin-coated thin films. Therefore, a shorter π−π stacking distance led to a better charge transport in FETs. Thus, FET devices with TGSS-treated active-channel arrays exhibited a high hole mobility and high on/off current ratio. This method proves to have a great potential for fabrication of conjugated polymers in organic electronic devices.

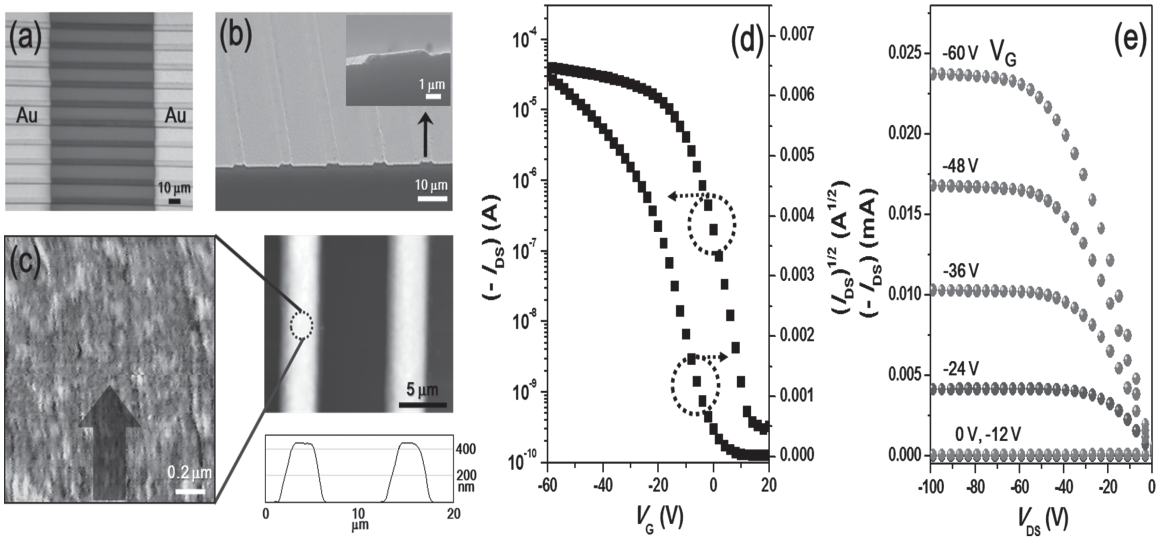

Figure 2 a) Optical microscopy image of micro-patterned prisms of PTDPP-DTTE between a pair of Au electrodes. b) SEM image of PTDPP-DTTE line patterns on a silicon wafer substrate. Inset: magnifi ed image of a single prism. c) AFM image (1.4 μm °ø 1.4 μm) of the upper surface of a prism, 2D image, and line profi le. Arrow indicates shearing direction. d) Transfer curves of FETs fabricated with TGSS micro-patterned prisms, which were thermally annealed at 200 °ΔC for 10 min. e) Output curve of PTDPP-DTTE micropattern device. * Sample : thermally annealed films [7]

Molecular Design

Semi-crystalline polymers like DPP have structural complexities which make it hard to understand the relationship of charge transport. Mobility in polymeric FETs is usually low due to the poor packing of molecules. Therefore, strengthening the intermolecular interactions between the neighboring molecules can enhance molecular orbital overlapping, which can be useful for charge carrier transport. Also, having a long-range crystalline order and right molecular orientation simplifies measuring charge transport and charge mobility. Polymers have finite length and their morphology comprises of ordered, nanocrystalline π –stacked lamellae separated by amorphous regions containing chain folds and chain ends that interrupt the idealized single-chain transport. Charges can therefore travel either along the lamellae by hopping between π-stacked chains, or travel perpendicular to the lamellae along individual chains [8]. Charge transport through amorphous region is due to the combination of hopping disordered segments and intrachain transport. Due to the complex interplay of inter and intrachain pathways it is difficult to discriminate whether mobility will be greater parallel or perpendicular to the lamellae.

Crossland, Ludwigs and coworkers were able to measure anisotropic charge transport mobility of moderately high molecular weight polymer like poly(3-hexylthiophene) P3HT (figure 3). Controlling the nucleation density to an extent, allowed FET channels to be placed within quasi-parallel lamellae with which

Crossland's team found that mobility was three times faster in the direction perpendicular to ordered π-stacked chains, despite the periodic amorphous regions [8]. The non-aligned boundaries formed where two growing crystals meet, act as barrier to charge carriers because of reduced tie-chains bridging adjacent ordered regions compared to boundaries between quasi-parallel lamellae. Thus, increasing the charge mobility relies on maximizing the intrachain transport component of ordered and disordered boundaries, controlling the number of non-aligned boundaries, and on placement and orientation of boundaries with respect to the transport direction.

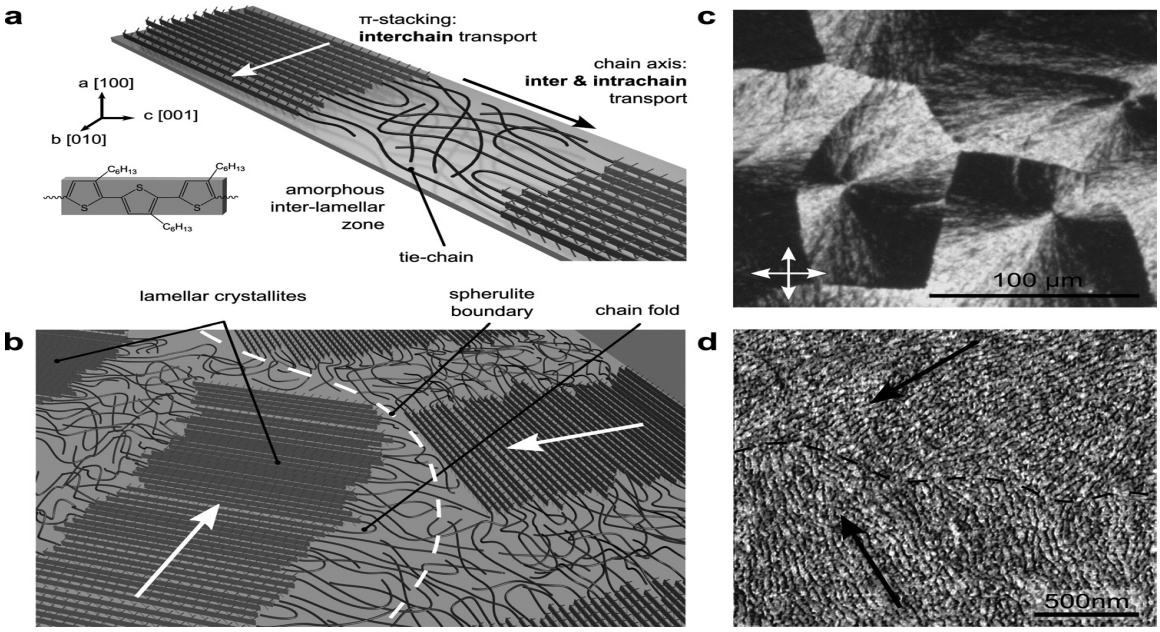

Figure 3 Molecular and crystalline morphology in P3HT films. a) Edge-on orientation of chains with side-chain (*a*-axis) standing parallel to the substrate normal form quasi-parallel nanocrystalline lamellae comprising π-stacked aggregates (solid rectangles) separated by amorphous zones with occasional tie-molecules spanning adjacent lamellae. b) Ordered regions at inter-spherulite boundaries are far less likely to be bridged by tie-molecules. c) Image of a spherulitic morphology at the micron scale in a 25 nm thick P3HT film crystallized at 83% *P*crystvap. d) Tapping-mode AFM image (phase contrast) of a meeting point of two spherulites. Radial growth directions and the approximate location of a spherulite boundary are highlighted in (b) and (d). The orientation and position of spherulite boundaries corresponds precisely with the structure visible in POM (data not shown) and confirms the nanocrystalline lamellar structure of the spherulite at the free surface [8]

DBT (DPP with 2 thiophene units) based polymers are made of electron-accepting DPP core with two electron donating thiophene units, that help to tune the highest occupied molecular orbital (HOMO) and lowest unoccupied molecular orbital (LUMO) energy levels, band gap, and film morphology. Two copolymers based on DBT (PVDT-8 and PVDT-10) having non-substituted thiophene-vinylene-thiophene (TVT) was reported by Chen and team. Their HOMO levels were lower than some of

the standard DPP based copolymers, which resulted in wider band gaps. Intermolecular interaction between the electron-donating TVT and electron-accepting DPP could shorten the distances between the polymer chains, which could lead to charge carrier transport [9]. PDVT-8 has short 2-octyldodecyl side-chains that showed mobility of 2.0–4.5 $cm^2\ V^{-1}\ s^{-1}$, with a current on/off ratio of 10^5–10^7, whereas PDVT-10 with long alkyl side chains exhibited a much higher mobility of up to 8.2 $cm^2\ V^{-1}\ s^{-1}$(figure 4), a current on/off ratio of 10^5–10^7. The interlayer and π- π stacking distances calculated from the XRD for PVDT-8 are 1.944nm and 0.372 nm, respectively, whereas for PVDT-10, the interlayer distance is about 2.111 nm and π- π stacking distance is 0.366nm [9]. Such small π- π stacking distances between polymer backbones suggests that strong intermolecular interaction exist, and that a longer side chain improves molecular ordering due to the easier polymer chain motion. Therefore, FETs based on PVDT-10 exhibit a high mobility of about 8.0 $cm^2\ V^{-1}\ s^{-1}$ that is higher than amorphous silicon FETs (0.1–1.0 $cm^2\ V^{-1}\ s^{-1}$).

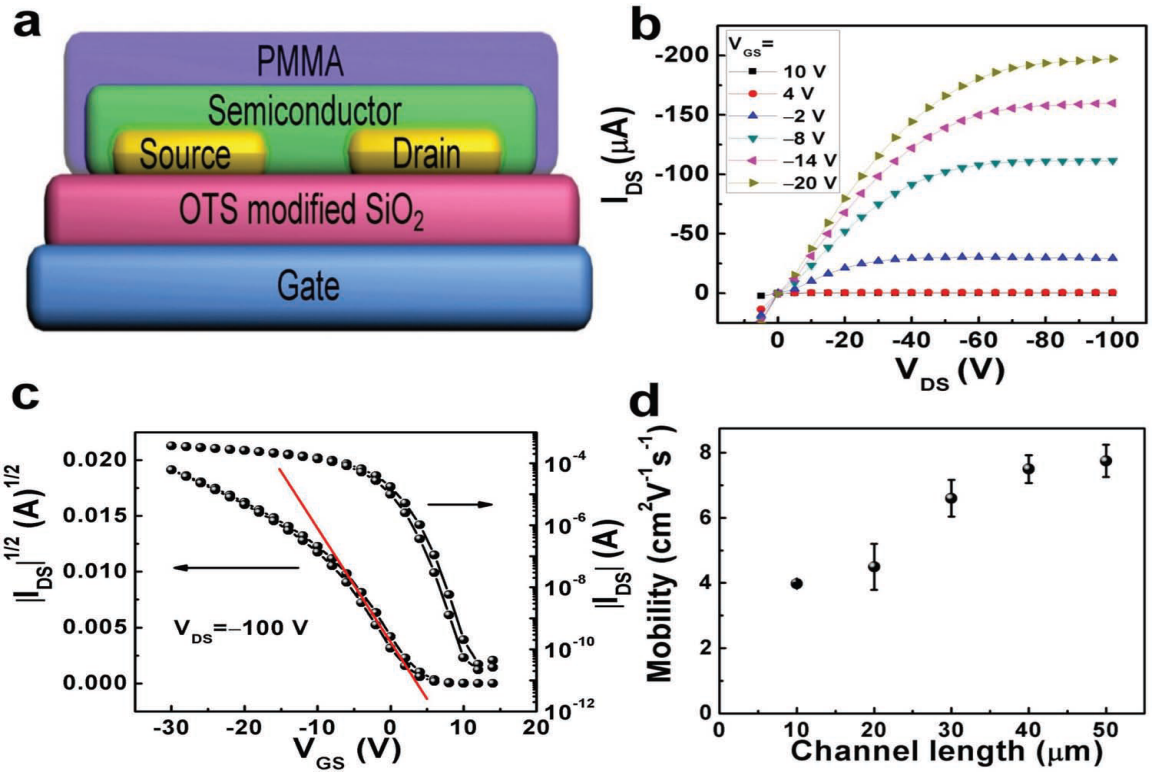

Figure 4 Device structure (a), output curves (b), and (c) transfer curves of PDVT-10 based OTFT devices (transistor dimensions: channel length (L) 1⁄4 0.05 mm; channel width (W) 1⁄4 1.4 mm). (d) shows the mobility distribution based on different channel lengths [9]**.**

Yuen, J et.al investigated the effects of donor – acceptor interaction by coupling DPP with neutral benzene (B), the weakly accepting benzothiadiazole (BT) and the strongly accepting benzobisthiadiazole (BBT). BBT- containing polymers have different properties compared to PBDPP and PBTDPP. BBT increases the LUMO values and decreases the HOMO values due to its accepting strength, resulting in easy injection of n-type and p-type charges, hence leading to bandgaps less than half of those of PBDPP and PBTDPP [10][11]. DPP coupled with BBT, forms strong ambipolar PBBT6DPP and PBBT12DPP, with p-type and n-type mobilities above 0.5

$cm^2V^{-1}s^{-1}$ and when coupled with B and BT, only p-type unipolar transport is noticed [10]. PBTDPP and PBBT12DPP have similar molecular weights (~9kD) and structural ordering with edge-on orientation and no π-stacking. Even with these similarities, PBBT12DPP has higher mobility, which is mainly because BBT moiety has a strong effect on interchain interactions. The strong interchain interactions occurring due to stronger interchain donor-acceptor (DA) interactions and the sulphur–nitrogen (S–N) intermolecular contact effects of benzobisthiadiazole, results in higher thermal stability, and better transport properties of PBT12DPP compared to PBTDPP. Figure 5 shows the transfer and output curves of typical devices of PBBTDPP, PBTDPP and PBDPP.

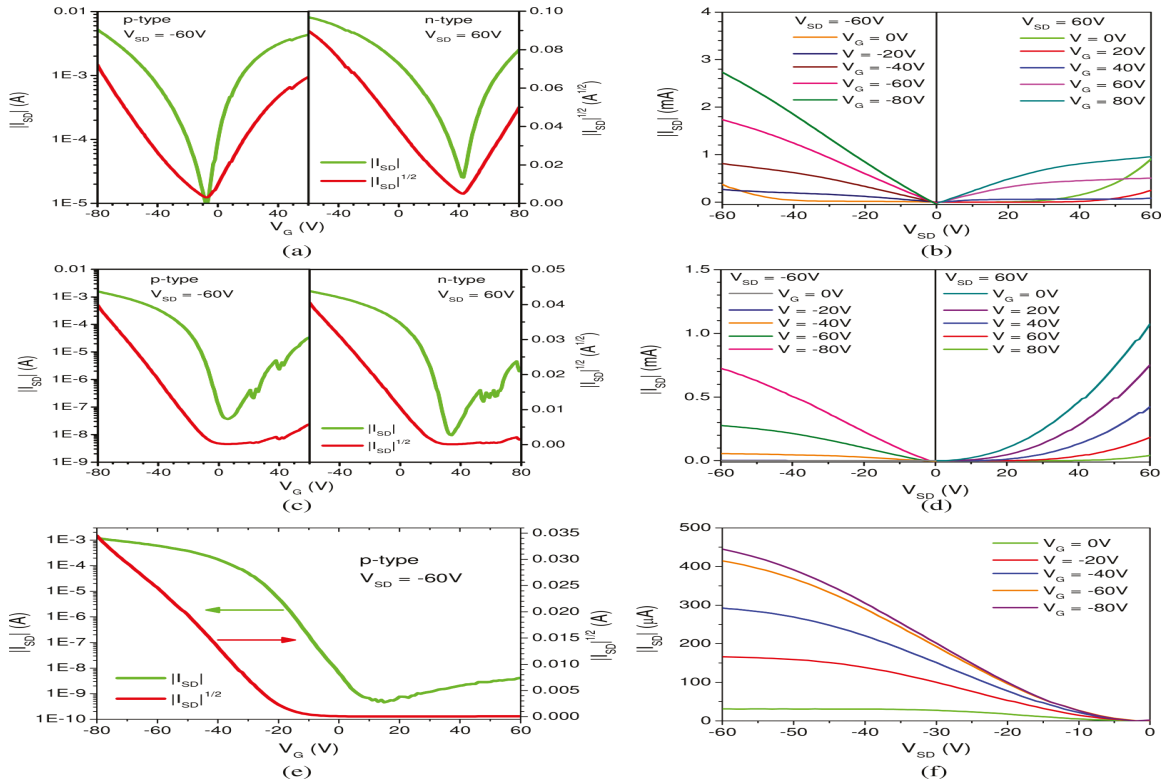

Figure 5 Typical transistor characteristics of PBBT12DPP, PBTDPP, and PBDPP at optimized annealing temperatures. a and b: Transfer and output characteristics, shown respectively, of a PBBT12DPP transistor annealed at 240 C with mobilities determined to be 1.1 cm2/(V s) for n-type transport and 1.0 cm2/(V s) for p-type transport. c and d: Transfer and output characteristics, shown respectively, of a PBTDPP transistor annealed at 200 C with p-type mobility determined to be 0.2 cm2/(V s). e and f: Transfer and output characteristics, shown respectively, of a PBDPP transistor annealed at 160 C with p-type mobility determined to be 0.17 cm2/(V s) [10].

Effect of Molecular Weight and Temperature

Significant progress has been achieved in the performance of solution-processed OFETs based on small molecules mixed with polymer semiconductors like DPP. For small molecule OFETs, however, crystallinity plays a crucial role to achieve a good device performance. Hole mobilities are much lower in small molecule OFETs due to difficulties in achieving high polymer organization. Closer intermolecular π−π stacking and increased macroscopic order can improve the hole mobility. It has been reported that regioregular versions of the D−A copolymer poly[4-(4,4-dihexadecyl-4H-cyclopenta[1,2-b:5,4-b′]-dithiophen-2-yl)-alt-[1,2,5]thiadiazolo[3,4-c]pyridine] (PCDTPT) show larger hole mobilities compared to similar polymers with less well-organized structural units [3]. Apart from molecular design, anisotropic order can be added during fabrication process by directional solvent evaporation of high molecular weight PCDTPT solutions on rubbed or nanogrooved substrates. The resulting PCDTPT layers in the tunnel-like configuration of field effect transistors showed random orientation on nonstructured surfaces. The fiber width varied between 30-40nm on nonstructured substrate and to 50-100nm for nanostructured substrates [3]. Wider the grooves, lesser the confinement for polymer alignment, and so 100nm structured substrates provided better polymer alignment.

Mobility also showed some dependence on annealing. Annealing 100-nm structured substrates at different temperatures yielded promising results with respect to

increasing the mobilities. Mobility increased from 1.9 to 2.6, 3.4, and 6.0 $cm^2/(V\ s)$ after annealing at 100, 150, and 200 °C, respectively [12]. A maximum mobility of 6.7 $cm^2/(V\ s)$ was noticed after using 100 nm structured substrate after annealing at 200 °C as shown in figure 6. No further increase is found when temperature is increased further. The alkyl stacking distance decreases due to dense conformation post annealing. Also, the long-range order increases and the interchain distance decreases post annealing which helps to lower the barrier for interchain hopping and increase charge mobility. Transfer and output characteristics are also shown in figure 6. Mobility also showed a dependence on the orientation of the fibers. Mobility along the fiber is higher than that perpendicular to fiber [12]. This is mainly because the polymer backbones are aligned along the fibers, due to which the carrier transport is high along the backbone direction. Thus, with proper orientation/alignment by using PCDTPT and thermal annealing, one can achieve higher hole mobility.

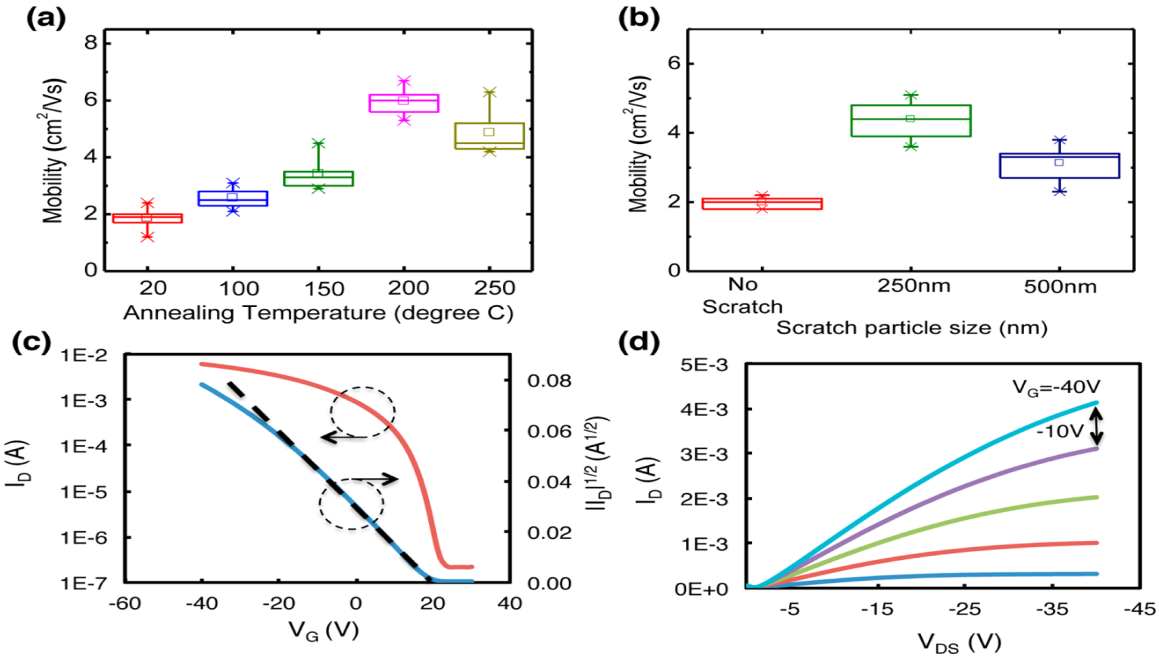

Figure 6 Mobility of PCDTPT devices. (a) Devices on 100-nm-structured substrates with various annealing temperatures and (b) devices on substrates without and with nanostructures after annealing at 200 °C. The horizontal lines in the box denote the 25th, 50th, and 75th percentile values. The error bars denote the fifth and 95 percentile values. The open square inside the box denotes the mean value. FET characteristics (I–V curves) of PCDTPT with a mobility of 6.7 cm2/(V s). (L = 20 μm, W = 1 mm) are shown in parts c and d: (c) transfer curves taken at VDS = −40 V and (d) output curves taken at various VG. The mobility values were calculated from the dashed lines in panel a. The contact resistance of this device is about 4000 Ω[12]

One important factor to achieve high carrier mobility in OFETs is the polymer molecular weight (MW). Low molecular weight materials have the tendency to form grain boundaries that reduces the carrier mobility significantly. Previously, it has been reported that high molecular weight materials exhibit high mobility. However, high MW materials are difficult to make and dissolve during fabrication process. Tseng and his group studied OFETs fabricated with PCDTPT of several MWs ranging from 30 to 300 kDa to understand the relationship between MW and carrier

mobility [3]. OFETs were fabricatied using the tunnel like configuration and regioregular PCDTPT on nanogrooved substrates as mentioned above. PCDTPT was separated into different MW fractions by gel permeation chromatography (GPC).

Carrier mobilities as a function of MW are shown in figure 7. Figure 7 summarizes data collected with FETs fabricated on normal substrates without nanogrooves and with nanogrooves. Average mobilities gathered from FETs without polymer chain alignment shows MW dependence, whereas higher MW gives higher carrier mobility. However, figure 7b shows that average mobilities are insensitive to MW when FETs are fabricated on nangrooved substrates. Thus, polymer orientation is important to achieve high mobility; in this case 50kDa polymer had the mobility of 23.7 $cm^2/(V\ s)$. Figure 7c and figure 7d show the transfer and output data. AFM characterization of PCDTPT (50 kDa) showed that polymer fibers are well aligned in one direction, with which the grain boundaries disappear, resulting in high carrier mobility. Transmission electron microscopy (TEM) using electron diffraction (ED) investigation further indicated that aligned polymer chains have "edge-on" orientation, thus enhancing the carrier mobility.

Temperature dependence of the mobility for OFETs with MW of 50, 160 and 300 kDa materials was also studied. For all 3 materials, the mobility was thermally activated with activation energy of 30 meV [3]. This low activation energy is due presence of no grain boundaries from chain-to-chain and implies that inter-chain hopping is efficient. Grazing incidence wide-angle X-ray diffraction (GIWAXS) to

understand the polymer order for different MW ranges was performed. Results showed that peaks were same for all the MWs, which means that the MW did not influence the structure. The crystalline correlation length (CCL) of alkyl stacking changes from 20 nm for 30kDa to 11nm for 300 kDa. However, the CCL of π−π stacking is ~4nm for polymers with different MW. This proved that carrier transport is mainly along the backbone of the chain with occasional hoping through π−π stacking to a neighboring chain [3]. Thus, the mobility is not dependent on MW, and higher mobility can be achieved by aligning polymer over long distances.

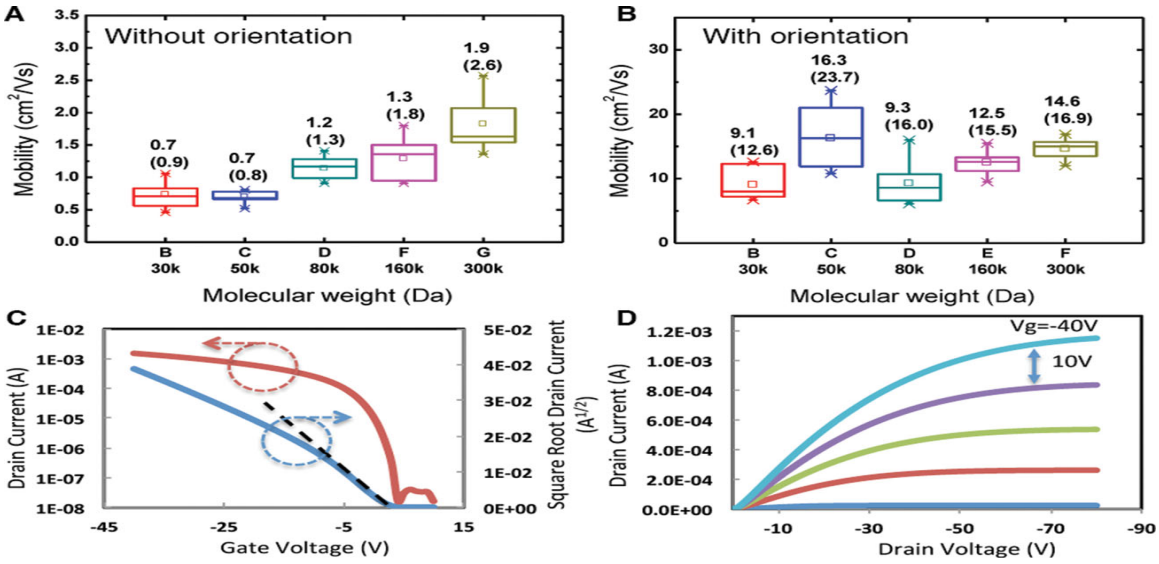

Figure 7 Mobility of PCDTPT OFETs after annealing at 200 °ΔC. The mobility value and the value in parentheses represent mean and maximum values obtained from 10 independent OFETs. (A) Devices fabricated by drop casting. (B) Devices fabricated by slow drying in the tunnel-like configuration. The horizontal lines in the box denote the 25th, 50th, and 75th percentile values. The error bars denote the 5th and 95th percentile values. The open square inside the box denotes the mean value. (C) and (D) FET characteristics of PCDTPT with mobility of 23.7 cm 2 /Vs. (L = 80 µm, W = 1 mm): (C) transfer curves taken at V DS = −80 V (D) output curves taken at various V G (0~−40 V)[3].

Interface Engineering

In order to increase the charge carrier mobility, smart side-chain engineering can be employed to polymer semiconductors. As discussed previously, polythiophene derivatives with edge-on structure exhibited high charge carrier mobilities. However, DPP based donor acceptor (D-A) polymers show higher carrier mobilities despite their low crystalline nature. This is mainly possible due to the highly polar nature of DPP, which allows for strong intramolecular and intermolecular charge transfer (CT) between the donor acceptor units. Moreover, smart adjustment of long-branched alkyl side chains can result in smaller intermolecular π−π stacking, and hence an increase of charge-carrier mobilities [13].

To test the above process, Kang and coworkers adjusted the branching position of poly[2,5-bis(2-decyltetradecyl)pyrrolo[3,4-c]pyrrole-1,4- (2H,5H)-dione-(E)-1,2-di(2,2′-bithiophen-5-yl)ethene] (P-24- DPPDBTE) and poly- [2,5-bis(2-decyltetradecyl)pyrrolo[3,4-c]pyrrole-1,4-(2H,5H)- dione-(E)-(1,2-bis(5-(thiophen-2-yl)selenophen-2-yl)ethene] (P-24-DPPDTSE) to get , P-29-DPPDBTE and P-29-DPPDTSE, in which branched alkyl chain has a longer alkyl spacer between the branching point and the backbone. Moving the branching position of the side chain away from the backbone of the DPP-based polymers resulted in short π−π stacking distance of 3.58 Å calculated by XRD analysis. Also, by using heat treatments, the maximum hole mobility was increased to as much as 12 $cm^2/(V \cdot s)$ [13].

UV-vis absorption spectra data collected during this study suggested that backbones of the polymers with the alkyl spacer have a planar structure due to steric hindrances from intermolecular π−π interactions.

FETs based on the P-24s and P-29s on OTS and Cytop-modified SiO_2/Si substrates were fabricated. Transfer characteristics of the devices are shown in Figure 8. FETs showed ideal, hysteresis-free transfer behavior for cytop-modified substrates, due to the fact that, polymer form defect-free interfaces with Cytop. Thus, Cytop-modified OFETs based on P-29s showed 2 or 3 times higher mobilities compared to P-24s, regardless of annealing conditions.

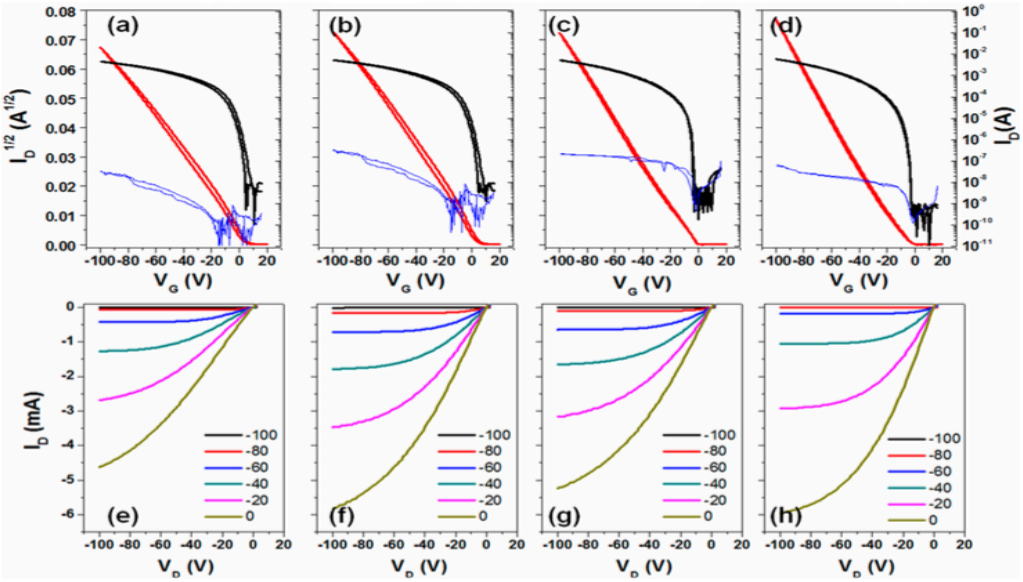

Figure 8 (Top) Transfer characteristics of FETs based on (a) P-29- DPPDBTE and (b) P-29-DPPDTSE fabricated with OTS-modified SiO_2/Si substrate. (c) and (d) correspond to Cytop-modified substrate for P-29-DPPDBTE and P-29-DPPDTSE, respectively. In each figure, blue curve represents leakage current. (Bottom) Output characteristics of FETs based on (e) P-29-DPPDBTE and (f) P-29-DPPDTSE fabricated with OTS-modified SiO_2/Si substrate. (g) and (h) correspond to Cytop-modified substrate for P-29-DPPDBTE and P- 29-DPPDTSE, respectively [13].

Chung, Kang and his coworkers have also addressed the issue of DPP-based polymer (PDPPDTSE) FETs showing anomalous transfer characteristics by deviating from linearity in the high gate-source bias regime. High gate-source bias (VG) brings the carriers close to the interface of the semiconductor/dielectric layers, which leads to charge trapping through the interfacial states [14]. This phenomenon is not seen in low-mobility organic semiconductors in which the density of the trap states is high. To further understand this effect, Poole-Frenkel constant was measured using the equation $m = m_{pre} \exp(gE)$, where m_{pre} is the prefactor mobility, E is the electric field along the charge carrier flow direction and g is the Poole–Frenkel constant. Poole-Frenkel constant (g) is related to trap states, which is determined by the width of DOS or hopping distance. The Poole-Frenkel constant measured at high V_G for PDPPDTSE in bottom contact FET device was higher than that measured at the low V_G regime. Hence, charge carriers in PDPPDTSE FETs experienced charge transport along broadened DOS at high VG. Although, the dielectric in the device was modified with OTS-18 SAM, the imperfection or the presence of local roughness degraded the mobility of the device. Thus, a new method to modify the dielectric layer was introduced, where SiO_2 was treated with Cytop layer, which is hydrophobic. No significant degradation in the transfer characteristics (figure 9) was noticed and the hysteresis behavior was decreased. These results indicate that the FET fabricated on a SiO_2/Cytop dielectric layer did not have a difference in the DOS between the bulk and the interface (figure 9), thus maintaining a high mobility.

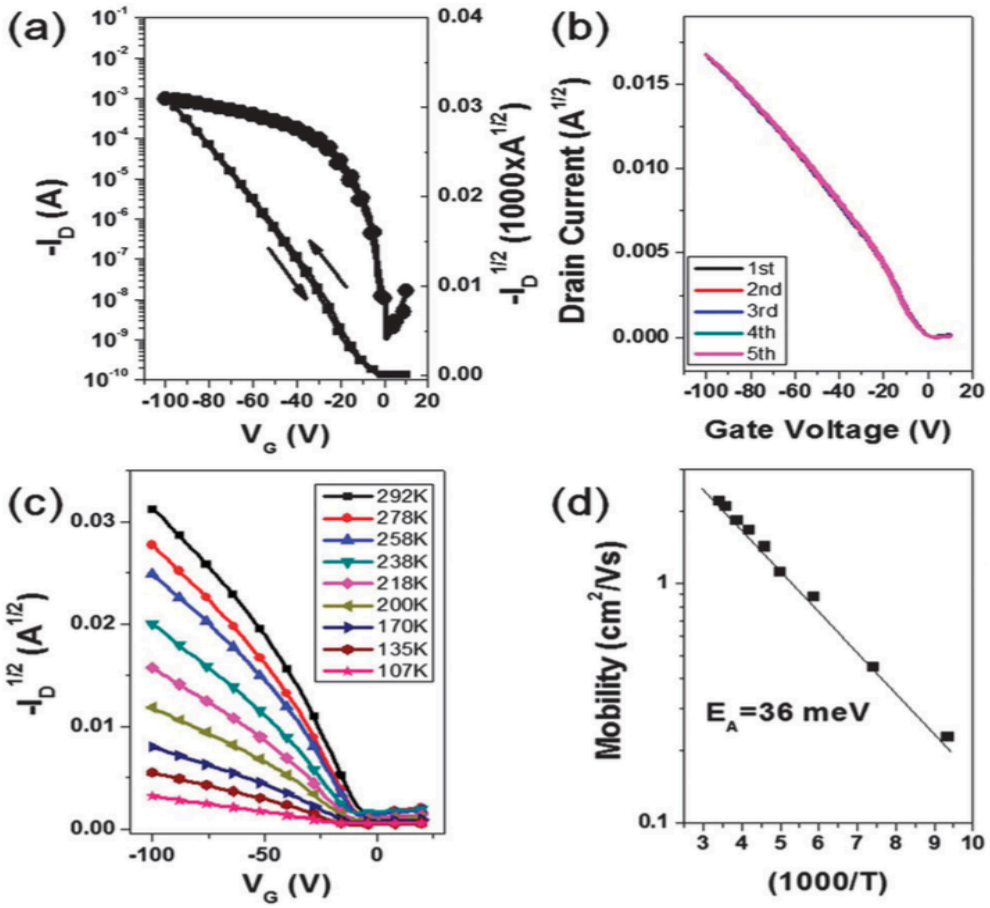

Figure 9 (a) Transfer characteristics of bottom-gate/top-contact FETs with SiO_2/ Cytop as the dielectric layer. (b) Repeated transfer measurements (c) Temperature dependence of transfer characteristics. (d) Arrhenius plot of obtained mobility with calculated activation energy [14]

Device Fabrication

Major advances have been made in improving the mobility of O-FETs by modifying various aspects of molecular design, interface engineering, and fabrication techniques as mentioned above. Having the right device structure also plays a key role in improving charge transport. High carrier mobility, high on/off current ratio, air stable operation etc are some of the key metrics that are needed for good performance of the device. Ha, T and his group reported a material combination and device geometry that included all of the key metrics mentioned above to enhance the performance of their device. They reported a device based on a furan-substituted DPP based polymer with bilayer gate dielectric that offered one of the best performances for DPP class of materials[15]. Furan when combined with DPP, provides high stability to the conjugated building blocks, even though Furan as an individual moiety is highly unstable[15]. Figure of merit (FOM) method was proposed to compare results of various transistor devices with respect to materials, device geometry and mobility.

Figure 10 shows the structure of furan-flanked diketopyrrolopyrrole–thienylene–vinylene–thienylene (PDPPFC24- TVT) polymer used in the device reported. The device has a recessed gate, present as a surface relief before the deposition of the gate insulator. The device also had a bilayer gate dielectric consisting of high –K oxide and low-k dielectric, which helped to improve mobility by reducing polaron effects and reduce density of interface traps. The

device had a channel width of 80 μm and a channel length of 4 μm, and the dielectric was treated with a self assembled monolayer (SAM) to enhance the molecular ordering, which helps with charge carrier injection and improved electrical contacts. The TFT device resulted in a field-effect mobility of 4.2 $cm^2\ V^{-1}\ s^{-1}$, a threshold voltage (V_{th}) of −1 V, an on/off current ratio of 1×10^7, and a sub-threshold swing (S.S.) of 0.3 V/decade when tested in ambient conditions [15]. The trap density of states calculated was about $5 \times 10^{12}\ cm^{-2}\ eV^{-1}$. Figures 11A and 11B illustrate that DPP-based polymers have the lowest activation energies for carrier densities less than $10^{13}cm^{-2}$. The activation energy of about 40meV is attained as the carrier concentration is increased which fits the multiple and thermal release (MTR) model.

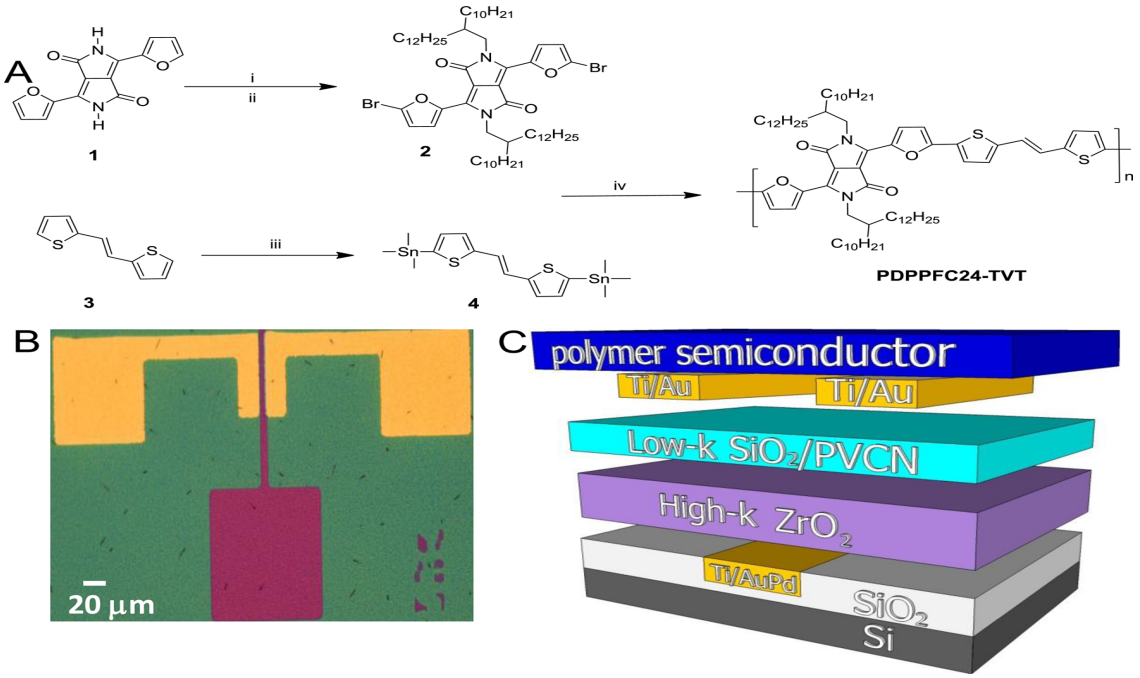

Figure 10 Device configuration of a recessed-gate DPP-based polymer TFT employing a bilayer of high-κ and low-κ dielectrics. PDPPFC24-TVT TFTs possessing a channel width of 80 μm and a channel length of 4 μm [15].

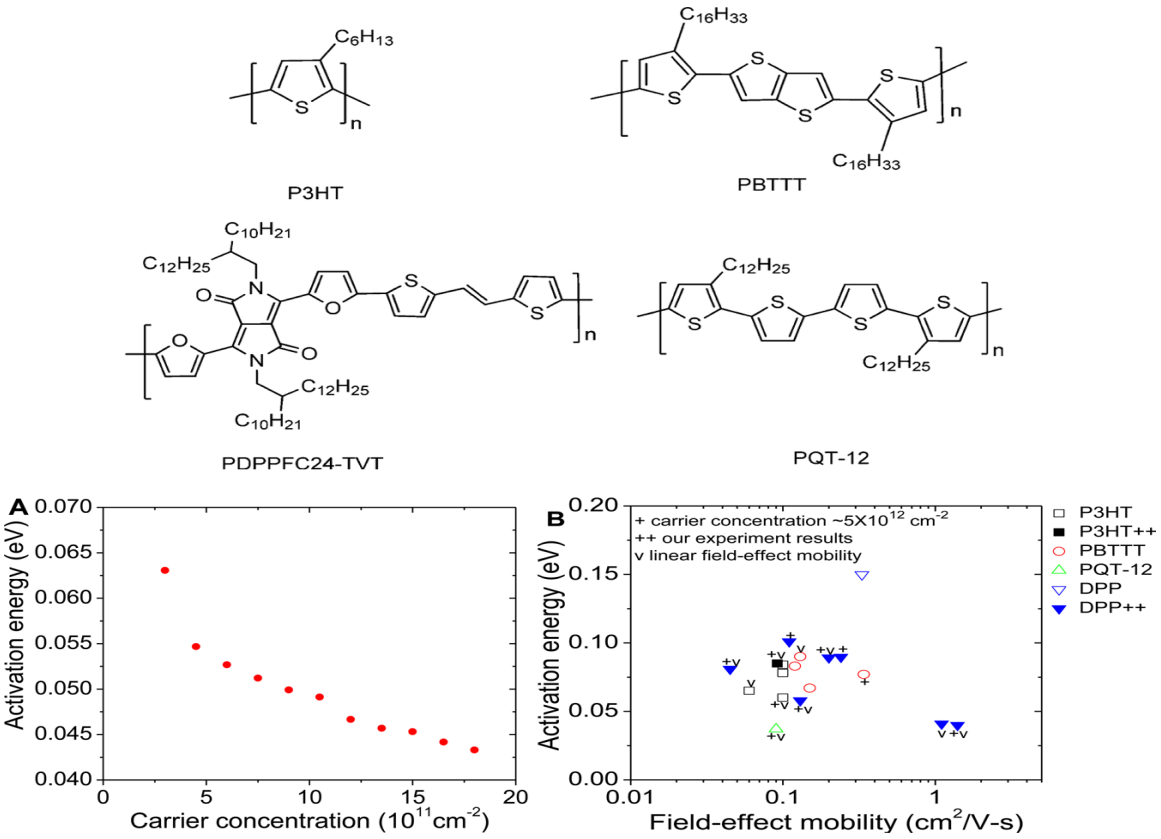

Figure 11 (A) Activation energies as a function of the channel carrier concentration in PDPPFC24-TVT TFTs. The magnitude of the lowest activation energy (~40 meV) is relatively small in comparison to measurements made with other DPP-based semiconductors and (B) activation energies as a function of field-effect mobility in various polymer semiconductor-based transistors [15]

FOM as a function of channel length and field effect mobility of various polymers was plotted (figure 12) to compare the field-induced channel conductivity per unit gate voltage. PDPPFC24-TVT used to fabricate the TFT device showed the highest FOM values, as it has one of the highest mobility for a small channel length (<10 μm) device compared to other materials.

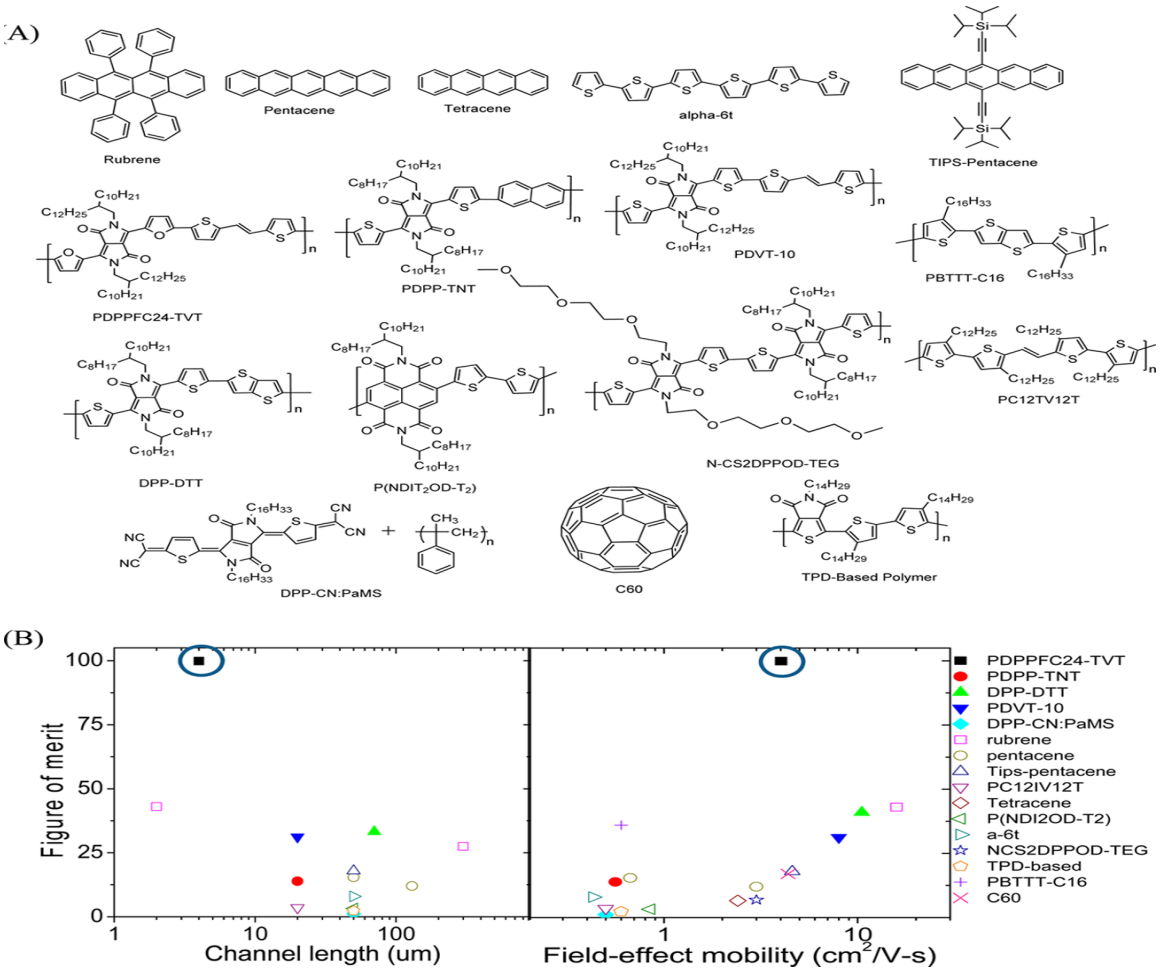

Figure 12 (A) Chemical structures of the compounds used for the FOM study and (B) FOM as functions of channel length and field-effect mobility on various organics and polymers to compare the gate field-induced channel conductivity per unit gate voltage, extracted by a product of mobility and the relative dielectric constant of the gate insulator [15]

Thus, this unique device geometry makes PDPPFC24-TVT a very important material for thin-film electronics and display applications.

Furthermore, a high electron mobility of up to 7.0 cm^2 V^{-1} s^{-1} is demonstrated by Hui-Jun Yun's group incorporating vinylene with DPP and nitrile group[16]. The

strong electron-withdrawing property of the nitrile group and its low steric-hindrance effect in the conjugation backbone, converts PDPP-TVT into an electron-dominant material.

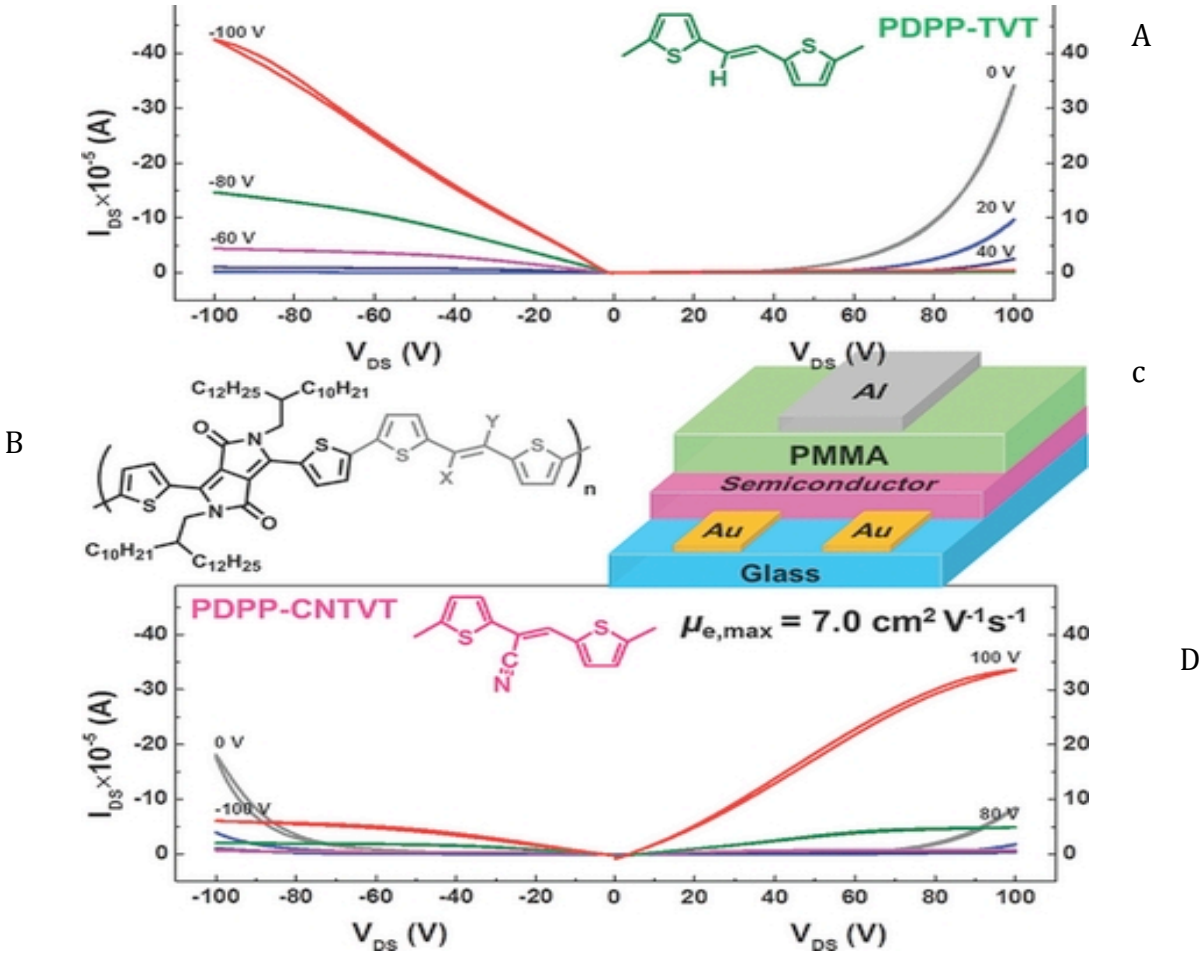

Figure 13 High electron mobility (up to 7.0 cm^2 V^{-1} s^{-1}) is demonstrated with a diketopyrrolopyrrole (DPP)-based semiconductor (PDPP-CNTVT) a) Transfer characteristics of PDPP-TVT b) Chemical structure of DPP-based semiconductor polymers for PDPP-TVT and PDPP-CNTVT c) schematic cross-section of top-gate/bottom-contact OFET structure, d) Transfer characteristics of PDPP-CNTVT [16]**.**

Tae-Jun Ha, Prashant Sonar and his team fabricated ambipolar organic FETs based

on diketopyrrolopyrrole-benzothiadiazole copolymer (PDPP-TBT) that gave mobility values of 0.53 $cm^2/V \cdot s$ for hole and 0.58 $cm^2/V \cdot s$ for electron in a top gate FET [17]. Combined effects of OTS-8 and PFBT surface treatments and thermal annealing played an important role in increasing the molecular ordering, resulting in better charge-carrier injection and transport. Moreover, the threshold voltage (V_{th}) of electrons and holes decreased considerably from 34.5 to 15.8 V and from −33.7 to −17.1 V in dual gate FETs. The transfer curves (figure 14) show good electrical performance of the device with 0.91V/dec of subthreshold swing (SS) and ON-OFF current ratios of 10^4[17].

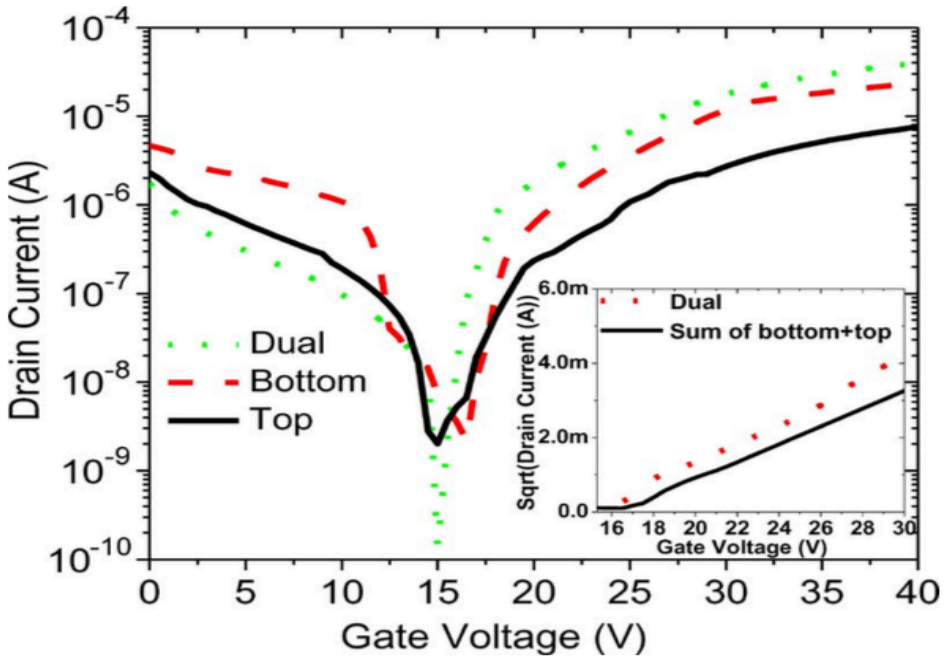

Figure 14 Transfer characteristics of ambipolar PDPP-TBT TFTs in top-, bottom-, and dual-gate modes. The inset shows that the current density from a dual gate is larger than the sum of both the top- and the bottom-gate mode operations [17]

Theino [3,2-b]thiophenediketopyrrolopyrrole-benzo[1,2-b:4,5-b′]dithiophene based co-polymer (PTTDPP-BDT) also exhibited ambipolar charge transport behavior, with maximum hole and electron motilities of 10^{-3} cm^2 V^{-1} s^{-1} and 10^{-5} cm^2 V^{-1} s^{-1}. X-ray diffraction measurements showed good π- stacking interactions and close molecular packing in the solid state [18]. Density functional theory calculations (DFT) showed that the HOMO was localized along the polymer backbone and LUMO on bis(thieno[3,2-b]thiophene)dike- topyrrolopyrrole units. DFT calculations explained the difference in hole and electron mobilities and also showed that the polymer backbone is almost planar. Aluminum electrodes were used as source and drain contacts in a bottom gate-top contact device creating ambipolar field-effect transistors. The transfer characteristics of this ambipolar PTTDPP-BDT device operated under different modes is shown in figure 15.

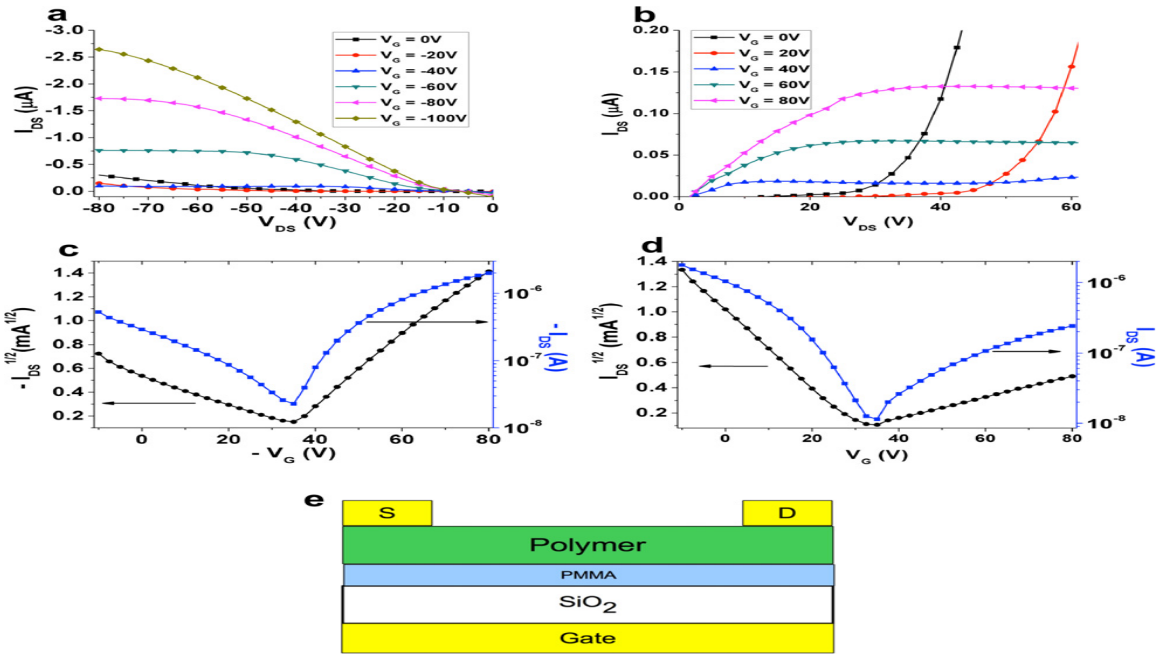

Figure 15 Output characteristics for a typical ambipolar PTTDPP-BDT based OFET with aluminum electrodes operating in (a) p-type mode; (b) n-type mode; (c) transfer characteristics for the OFET operating in p-type mode in the saturation regime (VDS = 80 V);(d) transfer characteristics for the OFET operating in n-type mode in the saturation regime (VDS = 60 V); (e) schematic of the OFET structure [source (S) and drain (D) electrodes] [18]

There is not enough research done on the use of non-functionalized DPP core with organic small molecules for the application of low-cost, low power consumption organic electronics. Palai et al. reported two non-functionalized soluble DPP derivates with only a solubilizing alky chain (DPP-R16 and DPP–R18) [19]. OFETs based on DPP-R16 (R = $C_{16}H_{33}$) and DPP-R18 (R = $C_{18}H_{37}$), were fabricated using solution (1D-microwire) and vacuum deposition.

The electrochemical properties studied using cyclic voltammetry and density functional theory (DFT) methods; Palai et al. calculated the HOMO and LUMO energy state. Both DPP-R16 and DPP-R18 had the HOMO energy level of 5.32eV, indicating that energy level depended on the conjugation system of DPP backbone with no effect of the long alkyl chain, whereas, LUMO energy levels of DPP-R16 and DPP-R18 was 3.43eV and 3.45eV. For a top contact field effect transistor, both DPP derivatives were prepared on a poly (4-vinylphenol) gate dielectric and gold (work function ~ 5.1eV) was used as a source/drain electrode [19]. The work function used is much closer to the HOMO energy levels compared to LUMO, which resulted in easier injection of holes and hence forming a p-channel characteristic.

Figure 16 shows the output and transfer characteristics of the OFET with DPP-R16 and DPP-R18. The output characteristics at different gate biases show p-type behavior for both devices. Charge accumulates near the channel region, with increasing the gate bias (V_{GS}), hence increasing the drain current. The transfer characteristics of OFETs with both DPP derivatives are shown in fig. 16c and 16d. The top contact OFET made with 1D- microwires of DPP-R18 showed field-effect mobility in the saturation region of 1.42 x $10^{-2}$$cm^2$/V s with I_{on}/I_{off} of 1.82 x 10^3[19]. Although, with the use of polymeric gate dielectric, the mobility is decreased by a considerable amount, the performance of DPP-R16 and DPP-R18 OFETs compared to that of functionalized DPP-based OFETs indicates that non-functionalized DPP

core with only side alkyl chain can be used as an active p-channel semiconductor for low cost organic electronic devices. This comparable device performance can be due to the high degree of crystallinity and molecular ordering in the thin-film.

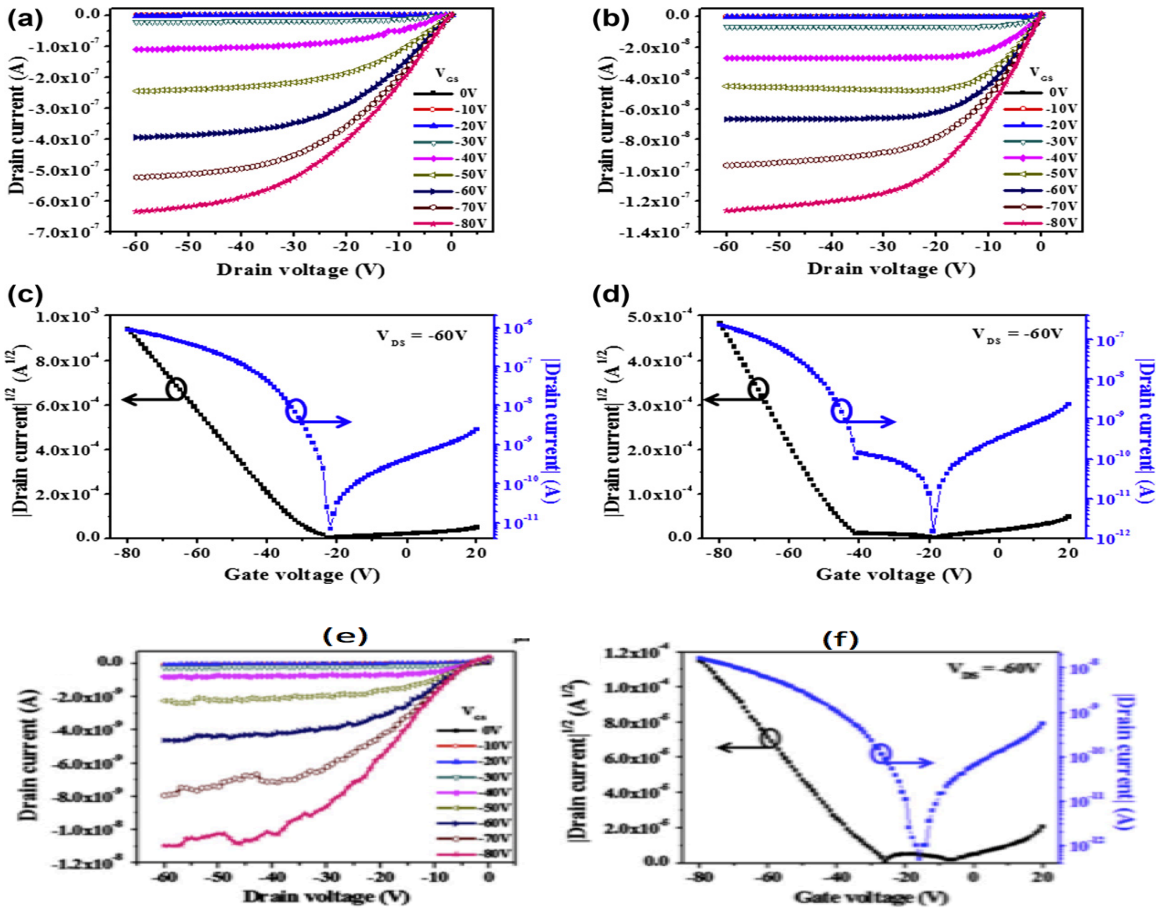

Figure 16 OFET characteristics of the DPP derivatives: (a and b) output curves of (VGS = from 0 to 80 V with a step of 10 V) DPP-R16 and DPP-R18 thin-film based devices; (c and d) transfer curves (VGS = from 20 to 80 V at fixed VDS = 60 V) of DPP-R16 and DPP-R18 thin-film based devices respectively. (e) Output (V_{GS} = from 0 to -80 V with a step of -10 V) and (f) transfer (V_{GS} = from 20 to -80 V at fixed V_{DS} = -60 V) characteristic (I_{DS} vs. V_{DS}) curves of OFETs based on DPP-R18 1D-microwires and 650 nm thick polymer gate dielectric. The channel length and width of the OFETs were 20 and 2.7 um, respectively [19][20]

DPPs cannot only be used as building blocks for organic semiconducting polymers and small molecules, but their hydrogen bonded (H-bonded) pigments can function as semiconductors as well. OFET devices were fabricated using a bottom-gate/top-contact configuration with anodically grown AlO_x passivated with tetratetracontane (C44H90, TTC) as dielectric. Glowacki et al. were able to measure ambipolar transport in three DPPs (Figure 17a): diphenyl–DPP (Pigment Red 255), di(p-chlorophenyl)–DPP (Pigment Red 254), and di(p-bromophenyl)–DPP (a frequent building block for DPP-containing polymers) [21]. Semiconducting properties of all the three materials are correlated with crystal structure, where an H bonded crystal lattice supports π- π stacking. Due to its smoother and more continuous morphology, p-Br-DPP was found to have the highest mobility for both carriers.

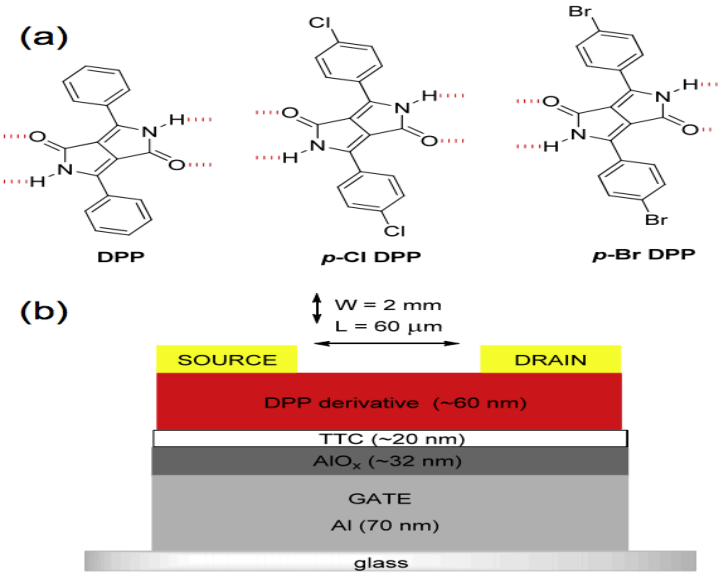

Figure 17 (a) Molecular structures of the three DPP derivatives used in this paper. Red dashed lines show where hydrogen bonds are formed with neighboring molecules. (b) Schematic of the OFET devices used in this study [21]**.**

Based on density functional theory calculations, the theoretical maximum ambipolar mobility values of 0.3 cm^2/V s was achieved. Though the mobility values remain low in comparison to other DPP-polymeric systems, the results show great promise in the application of H bonded crystal materials. Glowacki et al. suggests two possible ways to improve mobility in DPP derivatives (1) by decreasing the internal reorganization energy of electrons or holes by electron – withdrawing/donating substituents, and (2) by increasing the charge transfer integral by adding more H bonding functional groups. Thus, H-bonded DPPs can be a useful alternative to DPP-containing polymers where H-bonding is blocked by N-alkylation.

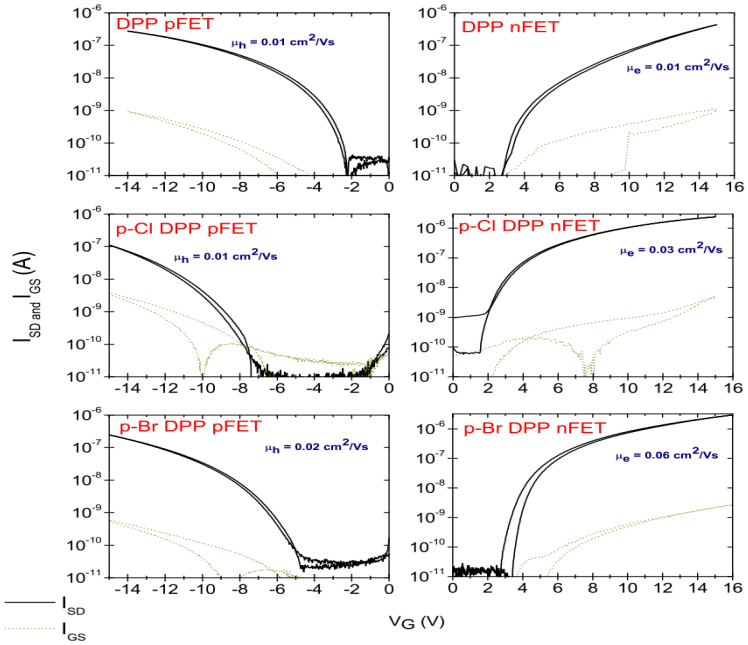

Figure 18 Transfer curves showing source–drain current (black traces), and gate leakage current (olive). Hole-enhanced devices shown in the column on the left were fabricated with Au source–drain electrodes, V_{SD} = -10 V in all cases. Electron-enhanced devices with Al source–drain electrodes are shown on the right, with V_{SD} = 10 V [21].

Conclusion

Since the first DPP-based polymer semiconductor for OTFTs was reported in 2008, many DPP-based polymers have been reported to show charge carrier mobility higher than 0.1 $cm^2 V^{-1} s^{-1}$. This report summarizes various DPP- containing polymers recently developed using different fabrication techniques and device architectures. Hole and electron mobilities reported in this paper are discussed in relation to properties such as short π- π stacking distance due to strong intermolecular interactions, alkyl substitution patterns and polymer molecular weights. Long branched side chains as in the case of PTDPP-DTTE, are required to substitute the DPP units to provide solubility. The substituents have profound effects on the coplanarity of the polymer backbone, the molecular organization and the thin film morphology. A lamellar structure with an edge-on orientation can be formed with or without thermal annealing during solution processing, which provides efficient charge transport in OFETs. In some cases, it has been shown that a high mobility can be achieved for DPP polymers even with face-on orientation. Performance of low performing DPP polymers can be improved by utilizing various techniques, such as by achieving a more ideal molecular weight, using optimal deposition and fabrication process and having an optimum device structure. Thus, these parameters play an important role in order to have efficient charge transport in DPP – based organic transistors.

Table 1 High mobility DPP-based compounds for OTFTs

Compound	Mn(kg /mol)	PDI	Hole Mobility ($cm^2/(V·s)$)	Electron Mobility ($cm^2/(V·s)$)	Ion/Ioff	Ref
PDPP3T	54	3.15	$4x10^{-2}$	$1x10^{-2}$	10^2 to 10^3	[22]
DPPT-T	104	3	$6x10^{-1}$	-	10^6	[23]
PDQT	25.4	2.39	$9.7x10^{-1}$		10^6	[24]
PBDPP	21	2.1	$2.7x10^{-2}$	-	10^6	[10]
PDBT-co-TT	89.7	2.36	$9.4x10^{-1}$	-	10^6	[2]
DPPT-TT	50	3.87	1.18	1.86	10^5 to 10^6	[25]
PDPP-TNT	63.7	1.43	$9.8x10^{-1}$	-	10^7	[26]
PDPPDTSE	30	2.1	2.8	-		[14]
PTTDPP-BDT	11.7	3.46	$6.2x10^{-4}$ $\pm 4x10^{-4}$	$8x10^{-5}$ $\pm 2x10^{-5}$	$3x10^1$ $\pm 1x10^1$	[18]
PBTDPP	9.4	1.6	$2.3x10^{-1}$	-	10^5	[10]
PBBT6DPP	8.7	1.5	$8.3x10^{-1}$	1.36	$10^2/10^2$	[10]
PBBT12DPP	8.81	1.8	0.89	0.9		[10]
PDPP-TBT			0.53	0.58	10^1 to 10^2	[17]
P-24-DPPDBTE	31	1.7	2.8	-	$>10^6$	[13]
P-24-DPPDTSE	33.5	1.78	4.4	0.84	$>10^6$	[13]
P-29-DPPDBTE	33.36	1.82	10.54	$7.1x10^{-2}$	$>10^6$	[13]
P-29-DPPDTSE	35.82	1.62	12.04	$3.9 x 10^{-1}$	$>10^6$	[13]
PDVT-8	70		2.0-4.5	-	10^5 to 10^7	[9]
PDVT-10	73.5		4.0-8.2	-	10^5 to 10^7	[9]
PCDTPT	-	-	23.7	-	-	[3]
PDPPFC24-TVT	-	-	4.2	-	10^7	[15]
PDPP-TVT	-	-		4.2	-	[16]
PDPP-CNTVT	-	-	-	7	-	[16]
DPP-R16	-	-	$1.13X10^{-2}$	-	10^3	[19]
DPP-R18	-	-	$4.77X10^{-3}$	-	10^4	[19]
PTDPP-DTTE	-	-	7.43	-	$>10^5$	[7]

Bibliography

[1] C. D. Dimitrakopoulos and P. R. L. Malenfant, "Organic thin film transistors for large area electronics," *Adv. Mater. (Weinheim, Ger.)*, vol. 14, no. 2, pp. 99–117, 2002.

[2] Y. Li, S. P. Singh, and P. Sonar, "A high mobility P-type DPP-thieno[3,2-b]thiophene copolymer for organic thin-film transistors," *Adv. Mater.*, vol. 22, no. 43, pp. 4862–4866, 2010.

[3] H.-R. Tseng, H. Phan, C. Luo, M. Wang, L. a Perez, S. N. Patel, L. Ying, E. J. Kramer, T.-Q. Nguyen, G. C. Bazan, and A. J. Heeger, "High-mobility field-effect transistors fabricated with macroscopic aligned semiconducting polymers.," *Adv. Mater.*, vol. 26, no. 19, pp. 2993–8, May 2014.

[4] J. E. Macdonald, M. Durell, D. Trolley, C. Lei, a. Das, P. C. Jukes, M. Geoghegan, a. M. Higgins, and R. a. L. Jones, "Applications of grazing incidence diffraction to polymer surfaces," *Radiat. Phys. Chem.*, vol. 71, no. 3–4, pp. 811–815, Oct. 2004.

[5] A. C. Arias, J. D. MacKenzie, I. McCulloch, J. Rivnay, and A. Salleo, "Materials and applications for large area electronics: solution-based approaches.," *Chem. Rev.*, vol. 110, no. 1, pp. 3–24, Jan. 2010.

[6] J. Li, Y. Zhao, H. S. Tan, Y. Guo, C.-A. Di, G. Yu, Y. Liu, M. Lin, S. H. Lim, Y. Zhou, H. Su, and B. S. Ong, "A stable solution-processed polymer semiconductor with record high-mobility for printed transistors.," *Sci. Rep.*, vol. 2, p. 754, Jan. 2012.

[7] J. Shin, T. R. Hong, T. W. Lee, A. Kim, Y. H. Kim, M. J. Cho, and D. H. Choi, "Template-guided solution-shearing method for enhanced charge carrier mobility in diketopyrrolopyrrole-based polymer field-effect transistors.," *Adv. Mater.*, vol. 26, no. 34, pp. 6031–5, Sep. 2014.

[8] E. J. W. Crossland, K. Tremel, F. Fischer, K. Rahimi, G. Reiter, U. Steiner, and S. Ludwigs, "Anisotropic charge transport in spherulitic poly(3-hexylthiophene) films.," *Adv. Mater.*, vol. 24, no. 6, pp. 839–44, Feb. 2012.

[9] H. Chen, Y. Guo, G. Yu, Y. Zhao, J. Zhang, D. Gao, H. Liu, and Y. Liu, "Highly π-extended copolymers with diketopyrrolopyrrole moieties for high-

performance field-effect transistors.," *Adv. Mater.*, vol. 24, no. 34, pp. 4618–22, Sep. 2012.

[10] J. D. Yuen, J. Fan, J. Seifter, B. Lim, R. Hufschmid, A. J. Heeger, and F. Wudl, "High performance weak donor-acceptor polymers in thin film transistors: effect of the acceptor on electronic properties, ambipolar conductivity, mobility, and thermal stability.," *J. Am. Chem. Soc.*, vol. 133, no. 51, pp. 20799–807, Dec. 2011.

[11] Y. Li, P. Sonar, L. Murphy, and W. Hong, "High mobility diketopyrrolopyrrole (DPP)-based organic semiconductor materials for organic thin film transistors and photovoltaics," *Energy Environ. Sci.*, vol. 6, no. 6, pp. 1684–1710, 2013.

[12] H.-R. Tseng, L. Ying, B. B. Y. Hsu, L. a Perez, C. J. Takacs, G. C. Bazan, and A. J. Heeger, "High mobility field effect transistors based on macroscopically oriented regioregular copolymers.," *Nano Lett.*, vol. 12, no. 12, pp. 6353–7, Dec. 2012.

[13] I. Kang, H. Yun, D. S. Chung, S. Kwon, and Y. Kim, "Record High Hole Mobility in Polymer Semiconductors via Side-Chain Engineering Record High Hole Mobility in Polymer Semiconductors via Side-Chain Engineering," no. c, 2013.

[14] D. S. Chung, I. Kang, Y.-H. Kim, and S.-K. Kwon, "Charge transport characteristics of a high-mobility diketopyrrolopyrrole-based polymer.," *Phys. Chem. Chem. Phys.*, vol. 15, no. 35, pp. 14777–82, Sep. 2013.

[15] T.-J. Ha, P. Sonar, and A. Dodabalapur, "Improved performance in diketopyrrolopyrrole-based transistors with bilayer gate dielectrics.," *ACS Appl. Mater. Interfaces*, vol. 6, no. 5, pp. 3170–5, Mar. 2014.

[16] H. Yun, S. Kang, Y. Xu, S. O. Kim, and Y. Kim, "Dramatic Inversion of Charge Polarity in Diketopyrrolopyrrole-Based Organic Field-Effect Transistors via a Simple Nitrile Group Substitution," pp. 7300–7307, 2014.

[17] D. Copolymer, "Characteristics of High-Performance Ambipolar Organic Field-Effect Transistors Based on a," vol. 59, no. 5, pp. 1494–1500, 2012.

[18] K. Tandy, G. K. Dutta, Y. Zhang, N. Venkatramaiah, M. Aljada, P. L. Burn, P. Meredith, E. B. Namdas, and S. Patil, "A new diketopyrrolopyrrole-based co-polymer for ambipolar field-effect transistors and solar cells," *Org. Electron.*, vol. 13, no. 10, pp. 1981–1988, Oct. 2012.

[19] A. K. Palai, H. Cho, S. Cho, T. J. Shin, S. Jang, S.-U. Park, and S. Pyo, "Non-functionalized soluble diketopyrrolopyrrole: Simplest p-channel core for organic field-effect transistors," *Org. Electron.*, vol. 14, no. 5, pp. 1396–1406, May 2013.

[20] A. K. Palai, J. Lee, S. Das, J. Lee, H. Cho, S.-U. Park, and S. Pyo, "A diketopyrrolopyrrole containing molecular semiconductor: Synthesis, characterization and solution-processed 1D-microwire based electronic devices," *Org. Electron.*, vol. 13, no. 11, pp. 2553–2560, Nov. 2012.

[21] E. Daniel, H. Coskun, M. a Blood-forsythe, U. Monkowius, L. Leonat, M. Grzybowski, D. Gryko, M. Schuette, A. Aspuru-guzik, and N. Serdar, "Hydrogen-bonded diketopyrrolopyrrole (DPP) pigments as organic semiconductors," vol. 15, pp. 3521–3528, 2014.

[22] J. Bijleveld, "Poly (diketopyrrolopyrroleâˆ' terthiophene) for Ambipolar Logic and Photovoltaics," *J. …*, pp. 6–7, 2009.

[23] X. Zhang, L. J. Richter, D. M. Delongchamp, R. J. Kline, M. R. Hammond, I. McCulloch, M. Heeney, R. S. Ashraf, J. N. Smith, T. D. Anthopoulos, B. Schroeder, Y. H. Geerts, D. a. Fischer, and M. F. Toney, "Molecular packing of high-mobility diketo pyrrolo-pyrrole polymer semiconductors with branched alkyl side chains," *J. Am. Chem. Soc.*, vol. 133, no. 38, pp. 15073–15084, 2011.

[24] Y. Li, P. Sonar, S. P. Singh, M. S. Soh, M. Van Meurs, and J. Tan, "Annealing-free high-mobility diketopyrrolopyrrole-quaterthiophene copolymer for solution-processed organic thin film transistors," *J. Am. Chem. Soc.*, vol. 133, no. 7, pp. 2198–2204, 2011.

[25] Z. Chen, M. J. Lee, R. Shahid Ashraf, Y. Gu, S. Albert-Seifried, M. Meedom Nielsen, B. Schroeder, T. D. Anthopoulos, M. Heeney, I. McCulloch, and H. Sirringhaus, "High-performance ambipolar diketopyrrolopyrrole-thieno[3,2-b]thiophene copolymer field-effect transistors with balanced hole and electron mobilities," *Adv. Mater.*, vol. 24, no. 5, pp. 647–652, 2012.

[26] P. Sonar, S. P. Singh, Y. Li, Z.-E. Ooi, T. Ha, I. Wong, M. S. Soh, and A. Dodabalapur, "High mobility organic thin film transistor and efficient photovoltaic devices using versatile donor–acceptor polymer semiconductor by molecular design," *Energy Environ. Sci.*, vol. 4, no. 6, p. 2288, 2011.

VITA

Kunal Mukesh Raghuwansi was born in Dubai, U.A.E. After finishing his high school in Dubai, he enrolled at Texas A&M University to pursue his bachelors in Biomedical Engineering. He received the degree of Bachelor of Science in August 2009. During the following years, he was employed as a biomedical engineer at NanoMedical Systems (NMS) in Austin, Texas. In January 2013, he decided to enter Graduate School at the University of Texas at Austin as a part time student while continuing to work for NMS.

Address: kraghuwansi@utexas.edu

This report was typed by Kunal Raghuwansi.